

## Optical properties of the pyrochlore oxide $\text{Pb}_2\text{Ru}_2\text{O}_{6.5}$

P. Zheng, N. L. Wang, and J. L. Luo

*Institute of Physics and Center for Condensed Matter Physics, Chinese Academy of Sciences, P.O. Box 603, Beijing 100080, China*

R. Jin and D. Mandrus

*Condensed Matter Sciences Division, Oak Ridge National Laboratory, Oak Ridge, Tennessee 37831, USA*

(Received 30 December 2003; revised manuscript received 4 March 2004; published 7 May 2004)

We present optical conductivity spectra for  $\text{Pb}_2\text{Ru}_2\text{O}_{6.5}$  single crystal at different temperatures. Among reported pyrochlore ruthenates, this compound exhibits metallic behavior in a wide temperature range and has the least resistivity. At low frequencies, the optical spectra show typical Drude responses, but with a knee feature around  $1000\text{ cm}^{-1}$ . Above  $20\,000\text{ cm}^{-1}$ , a broad absorption feature is observed. Our analysis suggests that the low frequency responses can be understood from two Drude components arising from the partially filled Ru  $t_{2g}$  bands with different plasma frequencies and scattering rates. The high frequency broad absorption may be contributed by two interband transitions: from occupied Ru  $t_{2g}$  states to empty  $e_g$  bands and from the fully filled O  $2p$  bands to unoccupied Ru  $t_{2g}$  states.

DOI: 10.1103/PhysRevB.69.193102

PACS number(s): 78.20.-e, 78.30.-j, 72.80.Ga

Pyrochlore compounds with general formula  $A_2B_2O_{7-\delta}$  are face-centered-cubic oxides with space group  $Fd\bar{3}m$  ( $A$  and  $B$  are cations). While  $B$  cation is sixfold coordinated and locates at the center of the distorted octahedra formed by corner  $O$  ions denoted as  $O(1)$ ,  $A$  cation is eightfold coordinated with six  $O(1)$  and two other oxygen ions  $O(2)$ . The  $BO_6$  octahedra are corner-sharing and compose a three-dimensional tetrahedral network, namely, the pyrochlore lattice. Intensive investigations of pyrochlore oxides have revealed a remarkable range of interesting and complex phenomena including colossal magnetoresistive effect, heavy fermion behavior, superconductivity, spin ice, spin glass and metal-insulator transition by selecting different  $A$  and  $B$  cations. Among those phenomena, the metal-insulator (MI) transition of ruthenates ( $B=\text{Ru}$ ) is unexpected and has thus attracted much attention.<sup>1-8</sup>

In general, the electron correlation degree of  $4d$  materials is smaller than that of  $3d$  materials and is thought to be within the intermediate-coupling regime. For pyrochlore ruthenates,  $A_2\text{Ru}_2\text{O}_{7-\delta}$ , the electrical properties show systematic change from a Mott insulator to a metal depending on  $A$  cation. For example,  $\text{Y}_2\text{Ru}_2\text{O}_7$  is an insulator;<sup>2</sup>  $\text{Tl}_2\text{Ru}_2\text{O}_7$  exhibits a metal-insulator transition at  $120\text{ K}$ ,<sup>3</sup> accompanied with a structural change from cubic to orthorhombic symmetry. Both  $\text{Pb}_2\text{Ru}_2\text{O}_{7-\delta}$  (Ref. 4) and  $\text{Bi}_2\text{Ru}_2\text{O}_{7-\delta}$  (Ref. 5) remain metallic from room temperature to the lowest measured temperature. It is found that metallic  $A_2\text{Ru}_2\text{O}_{7-\delta}$  has a greater Ru-O-Ru bond angle than those of insulating compounds.<sup>9</sup> The angle is affected by both  $A$  cation and oxygen vacancies  $\delta$  which are limited to  $O(2)$  site. While  $A$  cation may modify the Ru  $4d$  bandwidth by contributing some states to the total states near the Fermi level,<sup>1,6,8,10</sup> the oxygen vacancies, on the other hand, result in the partial oxidation of Ru cation, thus yielding smaller Ru-O distance compared to  $\delta=0$  case.

Optical spectroscopy is a powerful tool to probe the electronic structure and charge dynamics of a material. Several optical measurements have been performed on  $A_2\text{Ru}_2\text{O}_{7-\delta}$

compounds, which yield information about the effect of  $A$  cations on electronic structure. For  $\text{Tl}_2\text{Ru}_2\text{O}_7$ , a peak-like feature in the mid-infrared (IR) region was observed in the optical conductivity spectra,<sup>7</sup> which shifts to low frequencies with decreasing temperature. For  $\text{Bi}_2\text{Ru}_2\text{O}_{7-\delta}$ , the mid-IR feature moves to low frequency region further and overlaps with a sharp Drude component. In contrast, no mid-IR feature was observed in optical spectra of insulator  $\text{Y}_2\text{Ru}_2\text{O}_7$ . Thus, it appears that the mid-IR feature is related to the metallic nature of  $A_2\text{Ru}_2\text{O}_{7-\delta}$ . However, the origin of the mid-IR peak remains unclear. For  $\text{Tl}_2\text{Ru}_2\text{O}_7$ , the mid-IR peak is attributed to the interband transition between the lower Hubbard band (LHB) of Ru  $4d$   $t_{2g}$  energy level and the newly formed midgap state near the Fermi level caused by self-doping from  $\text{Tl}_2\text{O}$  to  $\text{RuO}_6$ .<sup>7</sup> For  $\text{Bi}_2\text{Ru}_2\text{O}_{7-\delta}$ , the electron-electron correlation is quite weak and its  $t_{2g}$  energy level could not split into LHB and UHB bands.<sup>11</sup> One may thus search for an alternative interpretation for metallic  $A_2\text{Ru}_2\text{O}_{7-\delta}$ .

$\text{Pb}_2\text{Ru}_2\text{O}_{7-\delta}$  is a Pauli paramagnetic metal in the whole measured temperature range.<sup>4</sup> Among reported pyrochlore ruthenates, this compound has the least resistivity. Its resistivity decreases significantly with decreasing temperature, whereas the resistivity of  $\text{Bi}_2\text{Ru}_2\text{O}_{7-\delta}$  keeps about  $600\ \mu\Omega\text{ cm}$  in the temperature range between  $10$  to  $300\text{ K}$ .<sup>5</sup> High-resolution electron-energy-loss spectroscopy (HREELS) analysis<sup>8</sup> shows that the density of states (DOS) at  $E_F$  of  $\text{Pb}_2\text{Ru}_2\text{O}_{7-\delta}$  is higher than that of  $\text{Bi}_2\text{Ru}_2\text{O}_{7-\delta}$ . All the above experimental phenomena imply that  $\text{Pb}_2\text{Ru}_2\text{O}_{7-\delta}$  is a better metal than  $\text{Bi}_2\text{Ru}_2\text{O}_{7-\delta}$ . In this article, we report the optical conductivity spectra of  $\text{Pb}_2\text{Ru}_2\text{O}_{6.5}$  single crystal at different temperatures. At low frequencies, the optical spectra show typical Drude responses, but with a knee feature around  $1000\text{ cm}^{-1}$ . Above  $20000\text{ cm}^{-1}$ , a broad absorption feature is observed. Our analysis suggests that the low-frequency responses may be understood from two Drude components arising from the partially filled Ru  $t_{2g}$  bands with different plasma frequencies and scattering rates. The high-frequency broad absorp-

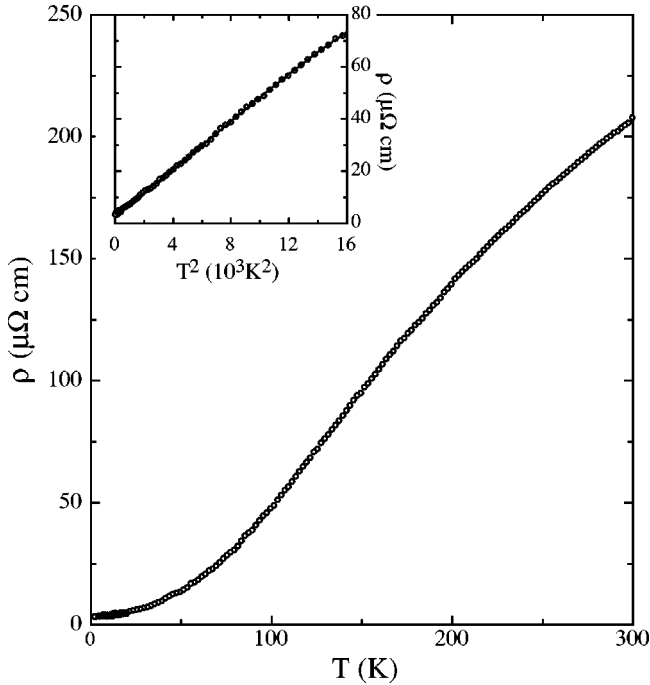


FIG. 1. Temperature dependence of the electrical resistivity  $\rho$  between 2 and 300 K. The inset is the plot of  $\rho$  vs  $T^2$  between 2 and 120 K. Note the linear behavior of  $\rho$  with  $T^2$ .

tion may be due to interband transitions from occupied Ru  $t_{2g}$  states to empty  $e_g$  bands and from the occupied O  $2p$  states to unoccupied Ru  $t_{2g}$  bands.

Single crystals of  $Pb_2Ru_2O_{7-\delta}$  were grown using a vapor transport method described in detail elsewhere.<sup>12</sup> X-ray diffraction results confirm the pyrochlore structure with the lattice parameter  $a = 10.252 \text{ \AA}$ . This suggests that the oxygen vacancy  $\delta \sim 0.5$  according to Ref. 13. The temperature dependence of the dc electrical resistivity, measured by standard four probe method, indicates a typical metallic behavior (see Fig. 1). The resistivity values are lower than the reported data,<sup>4</sup> reflecting high quality of the crystal. We selected a natural as-grown surface of the single crystal to measure the frequency dependent reflectivity  $R(\omega)$  from  $50 \text{ cm}^{-1}$  to  $30000 \text{ cm}^{-1}$  at different temperatures. The measurements were performed on a Bruker 66v/s spectrometer with a He flowing cryostat. An *in situ* overcoating technique is used for the reflectance measurement.<sup>14</sup> Standard Kramers-Kronig transformations are employed to derive the frequency-dependent optical conductivity.

Plotted in Fig. 2 are the reflectivity spectra at various temperatures. In low-frequency region, the reflectivity  $R(\omega)$  slightly increases with decreasing temperature. At higher but below  $8000 \text{ cm}^{-1}$  frequency region, the reflectivity slightly decreases with decreasing temperature.  $R(\omega)$  at different temperatures cross between  $1000 \text{ cm}^{-1}$  and  $2000 \text{ cm}^{-1}$ . The temperature dependent behavior of  $R(\omega)$  appears to be different from those of other strongly correlated metals, like  $La_{2-x}Sr_xCuO_4$ ,<sup>15</sup> perovskite titanates,<sup>16</sup> and MnSi,<sup>17</sup> all of which show the increase of reflectivity at least up to  $5000 \text{ cm}^{-1}$ . Those experimental results reflect the differences in their electronic structures and electron correlations. As we

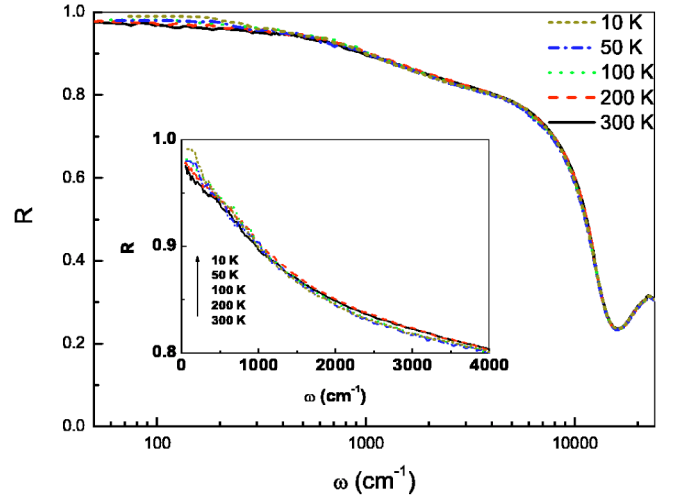


FIG. 2. (Color online) The plot of frequency-dependent reflectivities at 300 K, 200 K, 100 K, 50 K, and 10 K. Inset shows the low frequency data in an expanded scale.

shall see from the analysis of the conductivity spectra below, the change of the reflectivity with temperature in  $Pb_2Ru_2O_{6.5}$  can be essentially understood from two Drude responses. A plasma edge minimum can be seen at frequency close to  $13000 \text{ cm}^{-1}$ .

Figure 3 is a collection of the real part of the optical conductivity between 10 and 300 K. In the high frequency side, there is a broad interband transition peak at about  $23000 \text{ cm}^{-1}$ . Peaks at similar energies have been observed in  $Bi_2Ru_2O_{7-\delta}$  and  $Tl_2Ru_2O_7$ , and were attributed to the interband transition from filled O  $2p$  band to unoccupied Ru  $4d t_{2g}$  band. Since the transition from occupied  $t_{2g}$  band to empty Ru  $e_g$  band is also close to this energy,<sup>10</sup> this broad feature may compose of both interband transitions. Below  $13000 \text{ cm}^{-1}$ ,  $\sigma_1(\omega)$  shows a Drude-like response, but with a knee feature near  $1000 \text{ cm}^{-1}$ . Its spectra weight at about  $1000 \text{ cm}^{-1}$  decreases slightly when temperature decreases. In  $Bi_2Ru_2O_{7-\delta}$ ,<sup>18</sup> similar absorption feature at  $292 \text{ K}$  is ob-

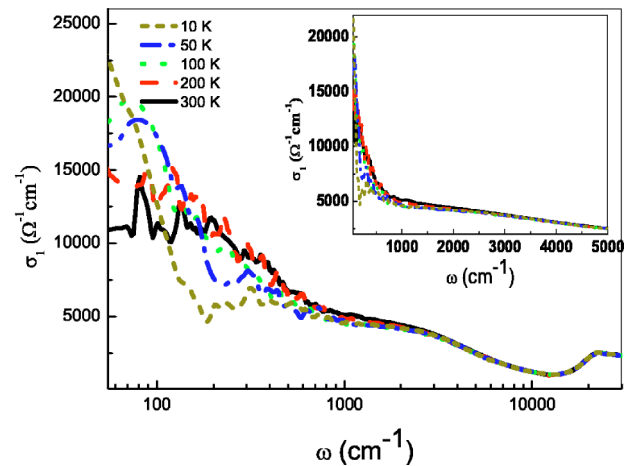


FIG. 3. (Color online) The plot of frequency dependent conductivities at 300 K, 200 K, 100 K, 50 K, and 10 K. Inset shows the low frequency data in an expanded scale.

served too, which is considered as a mid-IR peak of inter-band transition inherited from  $Tl_2Ru_2O_7$ .

The sum of the optical conductivity spectral weight gives a measure of the effective carrier number of  $Pb_2Ru_2O_{6.5}$ :

$$\frac{m_0}{m^*} N_{eff}(\omega_c) = \frac{2m_0 V_{cell}}{\pi e^2 N} \int_0^{\omega_c} \sigma(\omega) d\omega, \quad (1)$$

where  $V_{cell}$  is a unit cell volume,  $N$  the number of Ru ions per unit volume,  $m_0$  the free electron mass,  $m^*/m_0$  the ratio of the effective mass to free electron mass, and  $\omega_c$  the cutoff frequency. Assuming that  $\omega_c = 1.5$  eV (about  $12000 \text{ cm}^{-1}$ ) as for  $Tl_2Ru_2O_7$ ,<sup>7</sup> we get  $(m_0/m^*)N_{eff}(1.5 \text{ eV}) = 0.93$  for  $Pb_2Ru_2O_{6.5}$ , the value considerably higher than that for  $Tl_2Ru_2O_7$ . This is consistent with the fact that  $Pb_2Ru_2O_{6.5}$  is more metallic than  $Tl_2Ru_2O_7$ .

In optical conductivity spectra of  $Tl_2Ru_2O_7$ , there is a mid-IR peak centering at  $4000 \text{ cm}^{-1}$ .<sup>7</sup> Band structure calculations<sup>1</sup> show that antibonding states of  $Tl 6s$  and  $O(2) 2p$  lie in the energy range from  $-1$  eV to  $2$  eV and partly hybridize with the  $Ru 4d(t_{2g})-O(1) 2p$  antibonding states. That will lead to net charge transfer from  $Tl_2O(2)$  chain to the network of  $RuO(1)_6$  octahedra. Such a charge transfer effect will generate some midgap states within the gap between up Hubbard band (UHB) and low Hubbard band (LHB).<sup>7,19</sup> When the midgap states lie above  $E_F$  and close to LHB, an interband transition between LHB and those midgap states is possible. Then a Lorentz-like peak appears in the optical conductivity spectra. The previous explanation of the mid-IR absorption feature seen in  $Bi_2Ru_2O_{7-\delta}$  is on the similar basis, although it is considered that such self-doped state would be higher in metallic  $Bi_2Ru_2O_{7-\delta}$  than that in  $Tl_2Ru_2O_7$ .<sup>18</sup>

For  $Pb_2Ru_2O_{6.5}$ , both the dc resistivity (see Fig. 1) and the  $N_{eff}(\omega_c)$  deduced from our optical conductivity spectra show that it is a much better metal than  $Tl_2Ru_2O_7$ . Band calculations also show that the band structures of  $Bi_2Ru_2O_{7-\delta}$  and  $Pb_2Ru_2O_{6.5}$  around  $E_F$  are quite different from that of  $Tl_2Ru_2O_7$  due to different Ru-O-Ru angles and different ways of participation of A-cation orbits. The Ru-O-Ru angles in  $Bi_2Ru_2O_{7-\delta}$  and  $Pb_2Ru_2O_{6.5}$  are larger than that in  $Tl_2Ru_2O_7$ , leading to wider bandwidth of Ru  $4d$  band for  $Bi_2Ru_2O_{7-\delta}$  and  $Pb_2Ru_2O_{6.5}$  by changing the corresponding hopping integrals. The oxygen vacancies in  $Pb_2Ru_2O_{6.5}$  may result in a smaller Ru-O distance, as mentioned earlier, and as a result, would lead to further increase of the band width. Since partial Bi and Pb  $6p$  states situate near  $E_F$  and mix well with Ru  $t_{2g}$  states around  $E_F$ , the conducting electrons in  $Bi_2Ru_2O_{7-\delta}$  and  $Pb_2Ru_2O_{6.5}$  are more itinerant than that in  $Tl_2Ru_2O_7$ . Therefore, the on-site Coulomb interaction is relatively weak and the Hubbard bands merge into a single one.<sup>11</sup> In this case, the knee feature around  $1000 \text{ cm}^{-1}$  may not be attributed to the interband transition between LHB and the midgap states for  $Pb_2Ru_2O_{6.5}$ .

We note that the mid-IR feature for  $Pb_2Ru_2O_{6.5}$  has its central frequency at zero, suggesting a Drude characteristic.

TABLE I. The parameters of Eq. (2) at 300 K, 200 K, 100 K, 50 K, and 10 K.

$T(k)$	$\omega_{p,1}(\text{cm}^{-1})$	$\gamma_1(\text{cm}^{-1})$	$\omega_{p,2}(\text{cm}^{-1})$	$\gamma_2(\text{cm}^{-1})$
300 K	12779	349	40169	5902
200 K	13094	268	38983	5605
100 K	12190	140	38975	5543
50 K	11616	120	39160	5524
10 K	12158	31	39123	5268

Then we may consider the low frequency part of the optical conductivity of  $Pb_2Ru_2O_{6.5}$  as a sum of two kinds of intra-band transitions, i.e.,

$$\sigma_1(\omega) = \frac{1}{4\pi} \frac{\omega_{p,1}^2 \cdot \gamma_1}{\omega^2 + \gamma_1^2} + \frac{1}{4\pi} \frac{\omega_{p,2}^2 \cdot \gamma_2}{\omega^2 + \gamma_2^2}, \quad (2)$$

where  $\omega_{p,1}$  and  $\omega_{p,2}$  are the plasma frequencies, and  $\gamma_1$  and  $\gamma_2$  are relaxation rates of the free charge carriers. We find that this function can well reproduce all the spectral data at all temperatures we have measured. The fitting parameters are listed in Table I.

Figure 4 is the fitting result for spectral data at 50 K, where the thick solid line is the experimental data, the thin line is a fitting curve using Eq. (2), the dashed line is the first Drude term and the dotted line is the second Drude term.

Presented in Fig. 5 is a plot of the fitting curves of the first Drude term at different temperatures. The inset displays those of second Drude term. Both of them show usual narrowings with decreasing temperature. Our fitting results imply that two kinds of conducting charge carriers with different lifetimes have taken part in the intraband excitations, and have different temperature dependencies. The carriers with smaller  $\gamma$  value have stronger temperature dependence, which, therefore, dominates the dc resistivity, while another one is much weaker. The cooperation of the two different temperature-dependent behaviors leads to the decrease of the spectral weight around  $1000 \text{ cm}^{-1}$  in the optical conductivity spectra with decreasing temperature.

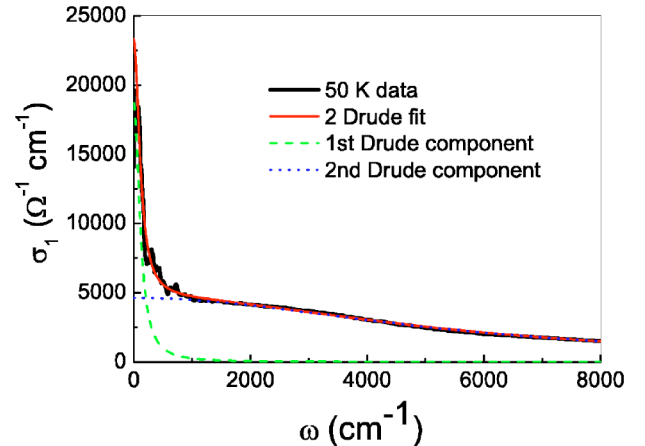


FIG. 4. (Color online) Fitting with two Drude terms to the optical conductivity spectrum at 50 K.

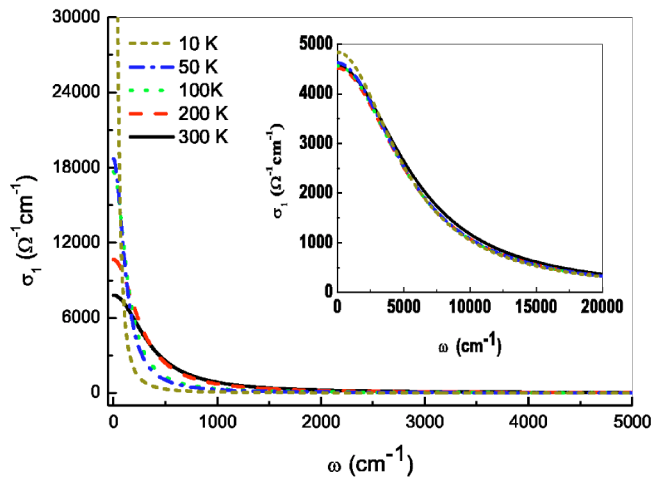


FIG. 5. (Color online) The temperature dependences of 1st Drude term and 2nd Drude term (in the inset) of the fitting function.

Our analysis is well consistent with the band-structure calculation results.<sup>10</sup> As displayed in Fig. 6, the fivefold degenerate Ru 4*d* levels are split, due to the octahedral crystal field, into an unoccupied  $e_g$  band which locate at 2–5 eV above  $E_F$ , and a partially occupied  $t_{2g}$  band between  $-1$  and  $1$  eV. This  $t_{2g}$  band is broadened by mixing with some Pb 6*p* states. The O 2*p* bands locate between  $-7.5$  eV and  $-2$  eV.<sup>10</sup> The broad feature at high frequencies (above  $20000\text{ cm}^{-1}$ ) is contributed by two possible interband transitions with similar energy scales: from the occupied Ru  $t_{2g}$

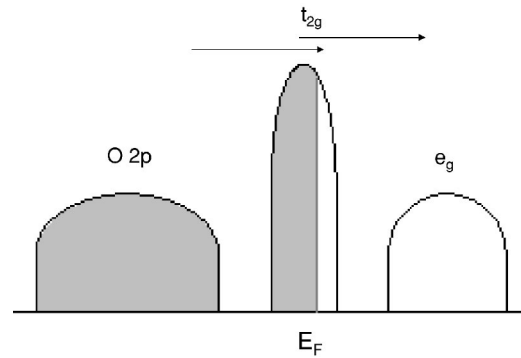


FIG. 6. A schematic picture of electronic states near  $E_F$  of  $Pb_2Ru_2O_{7-\delta}$ . The Ru 4*d* levels are split into  $t_{2g}$  and  $e_g$  bands. The partially occupied  $t_{2g}$  bands are hybridized with partial Pb 6*p* states. The filled O 2*p* bands are 2 eV away from the Fermi level.

bands to empty  $e_g$  bands and from the filled O 2*p* states to unoccupied Ru  $t_{2g}$  states. The low frequency part below the conductivity minimum is due to the intraband excitations of the two partially filled Ru  $t_{2g}$  bands. The existence of A-cation orbital near  $E_F$  actually leads to different band dispersions of the Ru  $t_{2g}$  bands.

This work is in part supported by National Science Foundation of China (No. 10025418, 10374109) and Wang-Kuan-Cheng Foundation for research collaboration (R.J.). Oak Ridge National Laboratory is managed by UT-Battelle, LLC, for the U.S. Department of Energy under contract DE-AC05-00OR22725.

- <sup>1</sup>F. Ishii and T. Oguchi, *J. Phys. Soc. Jpn.* **69**, 526 (2000).
- <sup>2</sup>M.A. Subramanian, G. Aravamudan, and G.V. Subba Rao, *Pro. Solid State Chem.* **15**, 55 (1983).
- <sup>3</sup>T. Takeda, M. Nagata, H. Kobayashi, R. Kanno, Y. Kawamoto, M. Takano, T. Kamiyama, F. Izumi, and A.W. Sleight, *J. Solid State Chem.* **140**, 55 (1998).
- <sup>4</sup>H. Kobayashi, R. Kanno, Y. Kawamoto, T. Kamiyama, F. Izumi, and A.W. Sleight, *J. Solid State Chem.* **114**, 15 (1995).
- <sup>5</sup>S. Yoshii and M. Sato, *J. Phys. Soc. Jpn.* **68**, 3034 (1999).
- <sup>6</sup>B.J. Kennedy, *Physica B* **241-243**, 303 (1998).
- <sup>7</sup>J.S. Lee, Y.S. Lee, K.W. Kim, T.W. Noh, Jaejun Yu, T. Takeda, and R. Kanno, *Phys. Rev. B* **64**, 165108 (2001).
- <sup>8</sup>P.A. Cox, R.G. Egdell, J.B. Goodenough, A. Hamnett, and C.C. Naish, *J. Phys. C: Solid State Phys.* **16**, 6221 (1983).
- <sup>9</sup>B.J. Kennedy and T. Vogt, *J. Solid State Chem.* **126**, 261 (1996).
- <sup>10</sup>William Y. Hsu, Robert V. Kasowski, Thomas Miller, and Tai-Chang Chiang, *Appl. Phys. Lett.* **52**, 792 (1988).
- <sup>11</sup>J.S. Lee, Y.S. Lee, T.W. Noh, K. Char, Jonghyurk Park, S.-J. Oh, J.-H. Park, C.B. Eom, T. Takeda, and R. Kanno, *Phys. Rev. B* **64**, 245107 (2001).
- <sup>12</sup>B. Rehak, M. Frumar, and L. Koudelda, *Cryst. Res. Technol.* **20**, 61 (1985).
- <sup>13</sup>H.S. Horowitz, J.M. Longo, and J.T. Lewandowski, *Mater. Res. Bull.* **16**, 489 (1981).
- <sup>14</sup>C.C. Homes, M. Reedyk, D.A. Crandles, and T. Timusk, *Appl. Opt.* **32**, 2973 (1993).
- <sup>15</sup>K. Takenaka, R. Shiozaki, S. Okuyama, J. Nohara, A. Osuka, Y. Takayanagi, and S. Sugai, *Phys. Rev. B* **65**, 092405 (2002).
- <sup>16</sup>T. Katsufuji and Y. Tokura, *Phys. Rev. B* **60**, 7673 (1999).
- <sup>17</sup>F.P. Mena, D. Van der Marel, A. Damasceli, M. Fath, A.A. Menovsky, and J.A. Mydosh, *Phys. Rev. B* **67**, 241101 (2003).
- <sup>18</sup>J.S. Lee, Y.S. Lee, K.W. Kim, T.W. Noh, J. Yu, Y. Takeda, and R. Kanno, *Physica C* **364-365**, 632 (2001).
- <sup>19</sup>M.B.J. Meinders, H. Eskes, and G.A. Sawatzky, *Phys. Rev. B* **48**, 3916 (1993).